

Accurate Measurement of Nano-Newton Thrust for Micropropulsion System Characterization

Andrew J. Jamison¹, Andrew D. Ketsdever², E.P. Muntz¹

¹ Department of Aerospace and Mechanical Engineering
University of Southern California
Los Angeles, CA 90089-1191

² Air Force Research Laboratory
Propulsion Directorate
Edwards AFB, CA 93524

IEPC-01-236

Abstract

The ability to measure extremely low thrust levels with unusual precision is becoming more critical as attempts are made to characterize the performance of emerging micropropulsion systems. Many new attitude control concepts for nanospacecraft involve the production of thrust below 1 μN . A simple, but uniquely successful thrust stand has been developed and used to measure thrust levels as low as 88.8 nano-Newtons with an estimated accuracy of $\pm 16\%$. Thrust levels in the range of 734 nano-Newtons to 1 μN have been measured with an estimated accuracy $\pm 2\%$. Thrust is measured from an underexpanded orifice operating in the free molecule flow regime with helium, argon, and nitrogen propellants. The thrust stand is calibrated using results from Direct Simulation Monte Carlo numerical models and analytical solutions for free molecule flow. The thrust stand exhibits a significant improvement in accurate, low thrust measurements compared to published results.

Nomenclature

A = area
 D = damping coefficient
 d = diameter
 F = force
 g = gravitational constant ($= 9.81 \text{ m/s}^2$)
 I = system inertia
 I_{sp} = specific impulse
 K = rotational spring constant
 k = Boltzmann's constant $= 1.38 \times 10^{-23} \text{ J/K}$
 Kn = Knudsen number
 \dot{M} = mass flow rate
 m = molecular mass
 n = number density
 p = pressure

R = distance from center of rotation to the point of applied force
 r = distance from LVDT to center of thrust stand rotation of the nNTS
 T = temperature
 t = time
 \mathfrak{S} = thrust
 x = linear deflection
 α = transmission probability
 λ = mean free path
 θ = angular deflection
 ω_n = natural frequency

subscripts

fm = free molecule
 o = stagnation region
 t = thruster or orifice

Introduction

The increasing need for thrust measurements below 1 μN stems from the development of nanospacecraft propulsion systems and missions requiring the precision matching of multiple thrusters. The next generation of nano- and pico-spacecraft will require uniquely capable propulsion systems for constellation formation and maintenance, attitude control, drag compensation and de-orbit maneuvers. Therefore, thrusters in the micro- and nano-Newton (nN) range will become an ever-increasing part of the aerospace industry. A uniquely successful nano-Newton Thrust Stand (nNTS) has been developed primarily to measure the thrust produced by microelectromechanical systems (MEMS) fabricated propulsion systems such as the Free Molecule Micro-Resistojet (FMMR).¹

To produce highly repeatable impulse bits on the order of 1 $\mu\text{N}\cdot\text{sec}$, the FMMR will produce low thrust which can act over a relatively long time. Long valve cycle times can improve the accuracy of impulse-bit delivery by minimizing errors associated with valve actuation. To produce an impulse bit of 1 $\mu\text{N}\cdot\text{sec}$, the FMMR will produce a steady state thrust of 100 nN over a 10 second period. The continued development of micropropulsion systems will, therefore, require highly accurate measurement techniques in the thrust range between 100 nN and 1 μN . Steady-state thrust measurements as low as 100 nN represent an improvement over state-of-the-art techniques of about 25 times based on currently published results.²

For larger propulsion systems, it is often necessary to match the performance of two or more thrusters very closely. For example, mission planners might require accurate knowledge of the thrust imbalance of two separate attitude control thrusters for a scientific mission. Ultimately, improvements in thrust stand resolution to 100 nN can have applications to all sizes of spacecraft thruster systems (i.e. not just micropropulsion).

Nano-Newton Thrust Stand

Previous investigations into extremely low thrust measurements have been hampered by facility vibrations, thrust stand drift, problems with gas and electrical connections, and calibration concerns.

Figure 1 shows the nano-Newton Thrust Stand (nNTS) which was designed to address many of the problems previously experienced in obtaining low thrust measurements. Overall, a design approach was taken that would develop a diagnostic tool that was simple to construct and operate. A torsion balance is perhaps the simplest configuration that can be utilized for steady-state or transient thrust measurements. As shown in Fig. 1, two flexure pivots are used to support the thrust stand and provide a restoring force. The pivots have a spring constant of approximately 0.0016 Nm/deg. The nNTS is completely symmetric about the center of rotation with two thrust armatures extending from each side of the stand. The thrust stand arms are approximately 25 cm long from the center of rotation. For thrust measurements below 1 μN , extensions were added to the thrust stand to provide larger deflections for a given thrust as shown in Fig. 2.

The thrust measurements involve sensing the angular displacement resulting from a torque applied to a damped rotary system. The present method for detecting angular deflection is to measure the linear displacement at a known radial distance using a Macro SensorsTM linear variable differential transformer (LVDT). The LVDT is an electromagnetic transducer that converts the rectilinear motion of an object into an electrical signal. The LVDT sensor is located approximately 19.7 cm from the center of rotation for the standard configuration and 61 cm from the center of rotation for the extended arm configuration. For a thrust level of 100 nN, the linear movement at the end of the extended configuration's arms is approximately 0.264 μm . Therefore, the error associated with the angular movement of the thrust stand armature is negligible.

As μN and nN thrust levels are approached, the connections of a thrust stand mounted thruster to its supply infrastructure become increasingly difficult to handle. The forces applied by these connections can be orders of magnitude larger than the thrust to be measured. Therefore, the most critical design constraint for sub- μN thrust measurements comes from not allowing direct mechanical connection of

propellant or power feed lines to the thrust stand. This was accomplished in the nNTS through the design of several liquid baths.

The purpose of the first liquid bath is shown schematically in Fig. 3. The bath of high viscosity oil serves two purposes for thrust stand operation. First, the oil acts as a gas seal whereby propellant fed into the inverted cylinder of the thrust stand can not escape into the surrounding vacuum except through the propulsion system. Liquid seals for gas containment have been investigated in previous research.³ With this configuration, propellant feed lines are not directly connected to the thrust stand. The propellant introduced into the thrust stand's inverted cylinder moves into the cylindrical arms and subsequently into the thruster's stagnation chamber. Second, the oil acts as a viscous damper for the thrust stand system. The level of viscous damping of the thrust stand can be changed by varying the height of the oil on the sides of the inverted cylinder. Great care was taken to identify an appropriate oil with high viscosity, low vapor pressure and negligible solubility for propellants of interest. The Dow Corning oil used has a viscosity of 10,000 C.S. and a specific gravity of 0.971 g/cm³.⁴

Results are presented here from the nNTS for thrust measurements as low as 89 nN. This represents the first time that thrust levels on this order have been accurately measured and reported. A unique calibration technique for thrust measurements below 1 μN is also presented. The calibration utilizes thrust measurements of thin walled, underexpanded orifices in the free molecule flow regime, corrected with results from analytical and Direct Simulation Monte Carlo (DSMC) numerical models.⁵ Extremely low, highly accurate thrust measurements are possible with the nNTS because of its unique design and calibration procedures.

Analysis

The thrust stand is a torsion balance with the oil bath acting as the viscous dampener of the system. The system can be characterized by a second order differential equation that accounts for the various moment contributions.

$$I\ddot{\theta} + D\dot{\theta} + K\theta = FR \quad (1)$$

For a rotational system as in the case of the nNTS, the spring constant K is in units of Nm/rad. The solution for the angular deflection of the nNTS can be derived as a function of time. For a steady-state thrust, F , the deflection is given as

$$\theta(t) = \frac{FR}{K} + \frac{FR}{K} e^{-bt} \sin(\omega_n t) \quad (2)$$

where

$$b = \frac{D}{2I} \quad (3)$$

and the natural frequency, ω_n , is

$$\omega_n = \sqrt{\frac{K}{I} - (b)^2} \quad (4)$$

The angular deflection of the thrust stand for the steady-state condition is

$$\Delta\theta = \frac{FR}{K} \quad (5)$$

Figure 4 shows a theoretical nNTS trace using Eq. (2). The initial deflection is nearly twice that of the steady-state condition, but the damping quickly reduces the oscillations to the steady-state thrust level from Eq. (5). Solutions to the equation of motion for torsional thrust stands with a transient impulse have been presented elsewhere.^{6,7}

For the case of the nNTS the angular movement of the armature is very small. The linear displacement measured by the LVDT can be found as

$$x = r \sin \theta \quad (6)$$

As previously mentioned, the thrust stand uses underexpanded orifices operating in the free molecule flow regime for calibration. For free molecule flow, the Knudsen number defined by

$$Kn_t = \frac{\lambda_o}{d_t} \quad (7)$$

is relatively high ($Kn \geq 10$). This is realized at very low stagnation pressures where the molecular mean free path is much larger than the orifice diameter. The free molecule mass flow, thrust and specific impulse are given by

$$\dot{M}_{fm} = \alpha m \frac{n_o \bar{c}'}{4} A_t = \alpha m n_o \frac{\sqrt{\frac{8kT_o}{\pi m}}}{4} A_t \quad (8)$$

$$\mathfrak{S}_{fm} = \alpha \frac{P_o}{2} A_t \quad (9)$$

$$Isp_{fm} = \frac{\sqrt{\frac{\pi k}{2 m} T_o}}{g} \quad (10)$$

Errors in the calculated thrust from Eq. (9) come from errors associated with the transmission probability, the measurement of the orifice area, and the measurement of the stagnation pressure.

For the orifice used here, the thickness to diameter ratio was $t/d = 0.015$. For thin walled orifices, the transmission probability α is very close to unity.⁸ Due to the small t/d of the orifice, the error in the calculated thrust associated with the assumption that $\alpha = 1$ transmission is approximately 1.5%.

Experimental Set Up and Procedure

The nNTS was installed in Chamber-IV of the Collaborative High Altitude Flow Facility (CHAFF-IV). CHAFF-IV is a 3 m diameter by 6 m long stainless steel vacuum chamber shown schematically in Fig. 5. Although CHAFF-IV is a cryogenically pumped, space simulation facility⁹, only a single diffusion pump was used for the reported experiments. The Zyrianka 900 diffusion pump has an ultimate pumping speed of 25,000 L/sec for nitrogen and 42,000 L/sec for helium. The ultimate facility pressure in CHAFF-IV is approximately 1.0×10^{-6} Torr with the single diffusion pump operating. The 1.0 m diameter diffusion pump is backed with a 2000 L/sec Roots blower system. The location of the thrust stand in CHAFF-IV relative to the pumping system and background inlet is also shown in Fig. 5. During experiments in CHAFF-IV, the

background pressure varied from 10^{-6} to 10^{-5} Torr over the range of operational stagnation pressures.

An underexpanded orifice was tested due to the simplified geometry and flow characteristics as compared to other systems, although the thrust stand was designed to support several complex micropropulsion devices. The orifices were conventionally machined in a tantalum shim with a diameter of $1 \text{ mm} \pm 0.025 \text{ mm}$ and a wall thickness of 0.015 mm ($t/d = 0.015$). The orifices were attached to aluminum plenums as shown in Fig. 6 with thrust vectors in opposite directions for increased deflection of the armatures. Nitrogen, helium, and argon were used as cold gas propellants at various stagnation pressures.

Pressure is measured, both in the nNTS's inverted cylinder and in the stagnation chamber of the orifice, with MKSTM 0.2 Torr pressure transducers. The propellant is introduced into the stagnation chamber of a thruster through an adjustable needle valve located downstream of an thermal, flow through mass flow meter. In the experimental configuration, the mass flow meter operated in the continuum regime throughout the pressure range studied.

Thrust measurements were obtained using the underexpanded orifice over the range of stagnation pressures from 8×10^{-4} to 1×10^{-2} Torr. Data for stagnation pressures in this range were taken with the nNTS using the extended armatures as shown in Fig. 2.

The signal from the thrust stand LVDT was sent to a 24-bit digitizing card. Since the digitizer voltage range was from -7.5 to $+7.5$ V, the associated bit noise from the digitizer is approximately $0.894 \mu\text{V}$. The LVDT that was used had a sensitivity of 260 mV/mm implying that the data acquisition system is limited to deflections several times greater than $3.4 \times 10^{-3} \mu\text{m}$. Figure 7a shows the bit noise from the data acquisition system without connection to the thrust stand LVDT. Figure 7b shows the digitizer signal with the LVDT connected to the thrust stand showing the zero-thrust noise environment experienced in CHAFF-IV. As indicated by the comparison of Figs. 7a and 7b, the noise environment experienced by the nNTS in CHAFF-IV is only slightly larger than the detection system bit noise.

Results and Discussion

The thrust stand deflection for helium propellant is shown in Fig. 8 as a function of the stagnation pressure over the range of $p_o = 8$ to 10 mTorr. Each data point in Fig. 8 represents the average of at least 5 individual test runs at a given stagnation pressure. The error in Fig. 8 is the $\pm \sigma$ error for all the tests at a given stagnation pressure, which represents the error in the repeatability of the measurement. Errors in the deflection measurement arise from errors in accurately measuring the stagnation pressure, thrust stand drift, and other anomalies in the thrust stand operation.

The Knudsen number ranges from approximately 20 to 167 for the helium flow in the pressure range shown in Fig. 8. Over this range, the flow can be considered free molecular, and the trend in the deflection (or thrust) versus stagnation pressure is expected to be linear as Eq. (9) indicates. Eq. (9) is independent of the propellant gas used assuming that the flow is in the free molecule range. Therefore, different propellants at the same stagnation pressure should produce the same free molecule (large Kn) thrust assuming that internal energy effects are negligible. The mean free paths for nitrogen and argon are approximately a factor of three lower for a given stagnation pressure, indicating that the analytical solution for the thrust from Eq. (9) is approximated for stagnation pressures less than 5×10^{-3} Torr (i.e. where $Kn \geq 10$). In all cases it was assumed that the gas temperature was within ± 1 K of the local ambient temperature, as established in separate tests of an operating thruster.

The effect of propellant gas in the free molecule range is shown in Fig. 9 for nitrogen, argon and helium propellants. For nitrogen and argon, the Knudsen number ranges from approximately 5 to 56 in the pressure range shown in Fig. 9. It is, therefore, expected that the deflection versus stagnation pressure for these free molecule flows should be nearly the same. The nitrogen free molecule thrust appears to be slightly higher than that for helium and argon at the same stagnation pressure which may indicate that internal energy is being added to the flow through rotation-translation collisional exchange.

Figure 10 shows a typical trace from the nNTS LVDT for a stagnation pressure of 7 mTorr. For Fig. 10(a), the armature was extended on only one side of the thrust stand with no mass balancing on the opposite side. For Fig. 10(b), both nNTS armatures were extended in an attempt to mass balance the stand. Both traces are for nitrogen gas at the same thrust level. The environmental noise in the data was reduced by a factor of 10 for the symmetric thrust stand configuration.

Calibration

The calibration of the nNTS for steady-state thrusts is complicated by the very nature of the extremely small forces being measured. Conventional methods of calibration such as hanging weights from an armature with a string/pulley system were attempted with little success. Typically small errors associated with the weight calibration scheme such as friction in the pulley/string system become increasingly important in the range of thrust below $1 \mu\text{N}$. For the accurate steady-state calibration of the nNTS below $1 \mu\text{N}$, a new technique was required.

The DSMC numerical model was used to obtain the thrust for the underexpanded orifice operating in the free molecule flow regime.¹⁰ The DSMC simulations used experimentally determined stagnation pressures, temperatures, and mass flows as boundary conditions. Table 1 shows the DSMC and analytically derived thrust from Eq. (9) for helium flow with Knudsen numbers greater than 20. As indicated in Table 1, the thrust derived from the DSMC method and analytical equation are in good agreement. The helium experimental results from Fig. 8 and the numerical results in Table 1 are used to generate the calibration plot in Fig. 11. As expected, the thrust stand deflection versus orifice thrust has a linear dependence. The linear calibration is found by the least-squared method for the helium data at high Knudsen numbers where the DSMC and analytical solutions are expected to be highly accurate. Different schemes and procedures were used to generate the calibration line; however, the error associated with these different procedures was found to be less than 1%.

The thrust generated by the orifice at high Knudsen number should be independent of the gas used for a given stagnation pressure, assuming that internal energy modes do not affect the thrust significantly.

Figure 12 shows the same calibration line shown in Fig. 11 plotted against the data for nitrogen and argon gases. As expected, the calibration line fits the nitrogen and argon data quite well. Figure 12 is used as a check on the applicability of the calibration factor for the orifice flow at high Knudsen number.

For future nNTS calibration, the use of the analytical thrust equation (Eq. (9)) is valid assuming the calibration orifice is operated at high Knudsen number. Since internal energy modes can create errors in the thrust determined by Eq. (9), monatomic gases such as helium and argon should be used for calibration. Future thrust stand operation will utilize an underexpanded orifice on one armature to provide in-situ calibration of the stand when propulsion systems are being tested as shown schematically in Fig. 3.

Error Analysis

For free molecule flow, the solutions obtained by the DSMC and analytical approaches are expected to be highly accurate. Sensitivity studies were performed with the DSMC to insure the solution was independent of grid spacing and number of simulated molecules.¹⁰ Therefore the error in thrust calibrations is approximately $\pm 12.6\%$ at the lowest helium thrust level due primarily to errors in measuring the stagnation pressure, the orifice diameter, and assuming a transmission probability of unity. The experimentally derived stagnation pressures, temperatures, and orifice diameter were used in the DSMC and analytical calculations as known parameters.

At the lowest helium stagnation pressure, $p_o = 8.5 \times 10^{-4}$ Torr, the error in the deflection calculated from the standard deviation is $\pm 9.5\%$. At $p_o = 6.93 \times 10^{-3}$ Torr, the standard deviation in the deflection data is $\pm 1.1\%$. Experimental error in measuring the thrust stand deflection comes from a variety of sources including errors in stagnation pressure measurement, system noise, and thrust stand drift. Although to some extent all of the sources of error are contained in the standard deviations quoted above, attempts were made to correct the measured deflection for the measured nNTS drift rate. The thrust stand drift rate was observed to be relatively constant over a particular steady-state thrust measurement, which allowed for straightforward correction. An example of the nNTS drift over a 5 minute steady-state thrust

measurement can be seen in Fig. 10. At the indicated 700 nN thrust level, the error associated with the drift was found to be less than 2%. At 88.8 nN, the error associated with the drift was approximately 15%. The errors associated with the nNTS drift were corrected in the final data analysis (e.g. Figures 11 and 12).

Table 2 shows the associated error in the thrust measurement expected at the two extremes of the data collected in this experimental study. For the helium data, the calibration from Table 1 and the error from Table 2 indicates that the lowest stagnation pressure $p_o = 8.5 \times 10^{-4}$ Torr produces a thrust of $88.8 \text{ nN} \pm 16\%$. At $p_o = 6.93 \times 10^{-3}$ Torr, the thrust is $734 \text{ nN} \pm 2\%$. Most of the error in the determination of the orifice produced thrust at low stagnation pressure comes from uncertainties in the pressure measurement and the scatter in the deflection data.

Facility Effects

It is known that the deflection for a given orifice stagnation pressure is dependent on the background pressure of the facility.¹¹ Figure 13 shows the measured deflection for nitrogen as a function of facility background pressure for several stagnation pressures. As seen in Fig. 13, the measured thrust tends towards the asymptotic limit at lower facility background pressures. For the range of stagnation pressures investigated in this study, the facility background pressure remained below 1×10^{-5} Torr. Therefore, the error in the thrust measurements associated with the facility background are assumed to be negligible.

Conclusion

For thrusts below $1 \mu\text{N}$, it has been shown that using the DSMC solutions for calibrating the thrust stand in the free molecule flow regime provides superior results to other methods. The use of a thin walled orifice allows for easy calibration since the free molecule nature of the gas flow can be easily determined and the analytical equations can then be applied with a reasonable level of certainty. Helium is used as the calibration gas for several reasons including having a relatively large Knudsen number for a given stagnation pressure and the fact that no internal energy modes enter into the determination of the thrust. For helium, a calibration line was

determined by using the DSMC thrust results and the experimental deflection correlated by the stagnation pressure. In addition, the helium calibration line was a close approximation for the argon and nitrogen data at similar Knudsen numbers. This method of calibration has the benefit of being easy to apply while having much improved accuracy over other methods in the range of thrust below $1\mu\text{N}$.

The nNTS exhibits a significant improvement in accurate, low thrust measurements compared to published results. The thrust range measured from the underexpanded orifice operating on a helium propellant was between $88.8\text{ nN} \pm 16\%$ and $734\text{ nN} \pm 2\%$. The data obtained with the thrust stand was extremely repeatable, and the nNTS design allowed for simple operation. The improved accuracy of the nNTS will allow for thrust characterization of many micropropulsion systems currently under development.

Acknowledgements

The authors are grateful to Prof. Deborah Levin and Ms. Alina Alexeenko (The Pennsylvania State University) for providing the DSMC calibration results. This work was supported by the Air Force Research Laboratory's Propulsion Directorate (PRSA).

References

1. Ketsdever, A.D., Wadsworth, D. C., Muntz, E.P., "Predicted Performance and Systems Analysis of the Free Molecule Micro-Resistojet," *Micropropulsion for Small Spacecraft*, edited by M. Micci and A. Ketsdever, Vol. 187, Progress in Astronautics and Aeronautics, AIAA Reston, VA, 2000, pp. 167-183.
2. Boccaletto, L., d'Agostino, L., "Design and Testing of a Micro-Newton Thrust Stand for FEEP," AIAA paper 2000-3268, July, 2000.
3. Muntz, E.P., "Pressure Measurements in Free Molecule Flow with a Rotating Arm Apparatus," UTIA TN 22, 1958.
4. Tew, J., VanDenDriessche, J., Lutfy, F., Muntz, E.P., Wong, J., Ketsdever, A., "A Thrust Stand Designed for Performance Measurements of the Free Molecule Micro-Resistojet," AIAA paper 2000-3673, July, 2000.
5. Bird, G.A., *Molecular Gas Dynamics and the Direct Simulation of Gas Flows*, Clarendon Press, Oxford, England, 1994, pp. 208-217.
6. Haag, T.W., "Thrust Stand for Pulsed Plasma Thrusters," *Review of Scientific Instruments*, Vol. 68, No. 5, 1997, pp. 2060-2067.
7. Cubbin, E.A., Ziemer, J.K., Choueiri, E.Y., Jahn, R.G., "Pulsed Thrust Measurements Using Laser Interferometry," *Review of Scientific Instruments*, Vol. 68, No. 6, 1997, pp. 2339-2346.
8. Livesey, R., "Flow of Gases Through Tubes and Orifices," *Foundations of Vacuum Science and Technology*, edited by J. Lafferty, John Wiley and Sons, New York, 1998, pp. 81-140.
9. Ketsdever, A.D., "Design Considerations for Cryogenic Pumping Arrays in Spacecraft-Thruster Interaction Facilities," *Journal of Spacecraft and Rockets*, Vol. 38, No. 3, 2001, pp. 400-410.
10. Alexeenko, A.A., Levin, D.A., Gimelshein, S.F., Ivanov, M.S., Ketsdever, A.D., "Numerical and Experimental Study of Orifice Flow in the Transitional Regime," AIAA paper 2001-3072, June, 2001.
11. Ketsdever, A., Muntz, E.P., "Facility Effects on Performance Measurements of Micropropulsion Systems," AIAA paper 2001-3335, July, 2001.

P_0 (mTorr)	K_n	\mathfrak{S} (nN) (DSMC)	\mathfrak{S} (nN) (analytical)
0.85	167.1	88.88	88.98
1.38	102.9	145.1	144.4
2.05	69.3	216.2	214.6
3.39	41.9	358.4	354.9
5.15	27.6	545.2	539.1
6.93	20.5	734.1	725.5

Table 1: Free molecule calibration data for helium.

\mathfrak{S} (nN)	DSMC calibration error			Experimental Error	
	Error in α	Error in d_0 (mm)	Error in p_0 (mTorr)	Deflection $\pm \sigma_D$ (%)	Thrust $\pm \sigma_3$ (%)
88.8	1.0 ± 0.015	1 ± 0.025	0.85 ± 0.1	9.5	16.1
734	1.0 ± 0.015	1 ± 0.025	6.93 ± 0.1	1.1	2.0

Table 2: Errors contributing to the thrust error.

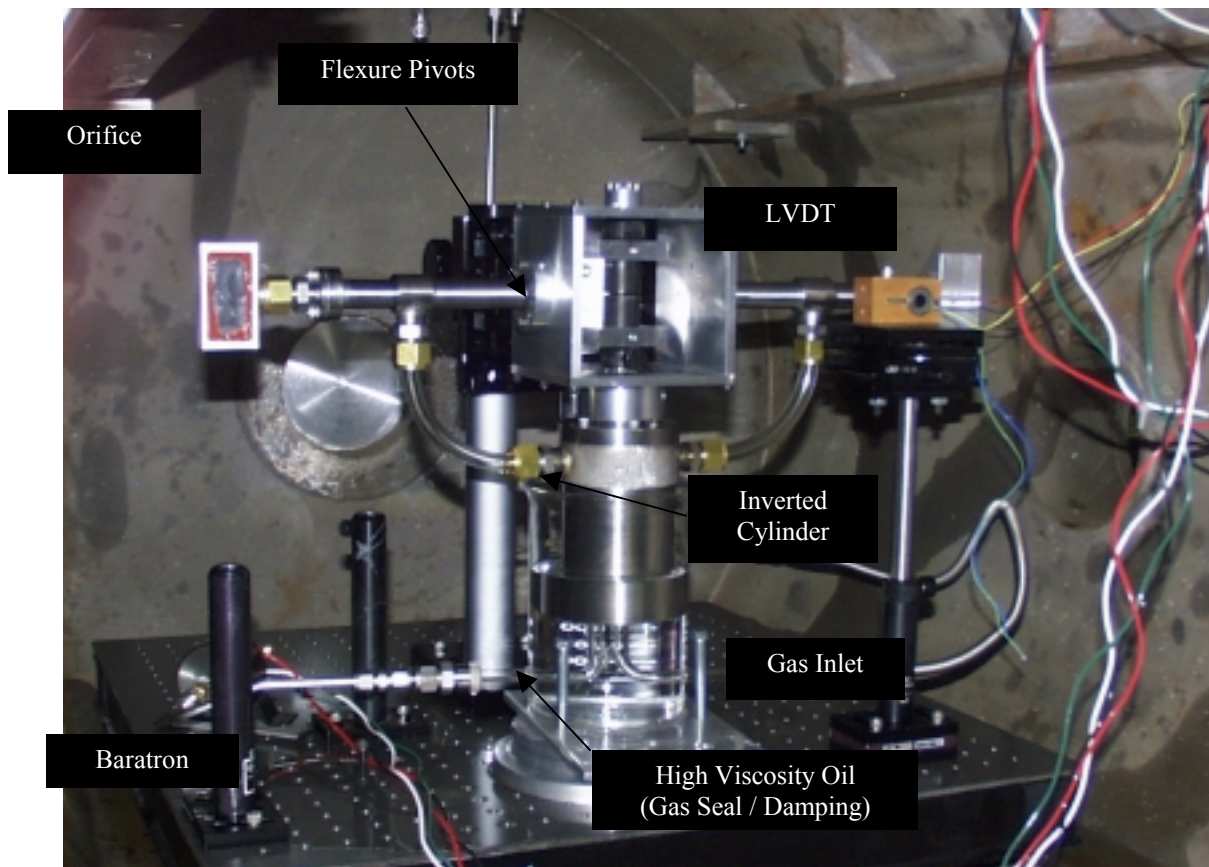


Figure 1: The nano-Newton Thrust Stand (nNTS) installed in a vacuum chamber.

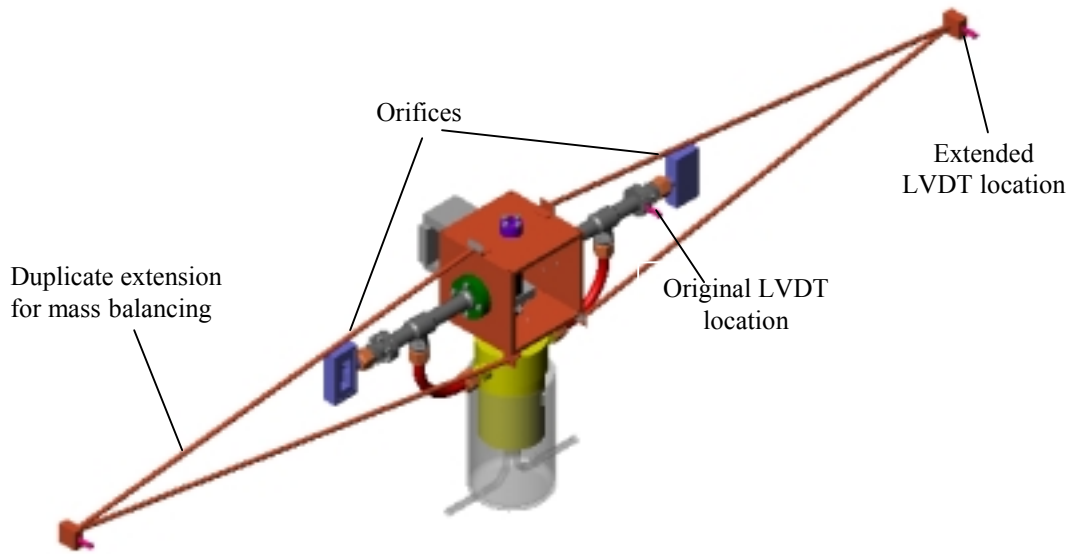


Figure 2: The nNTS with extended armatures.

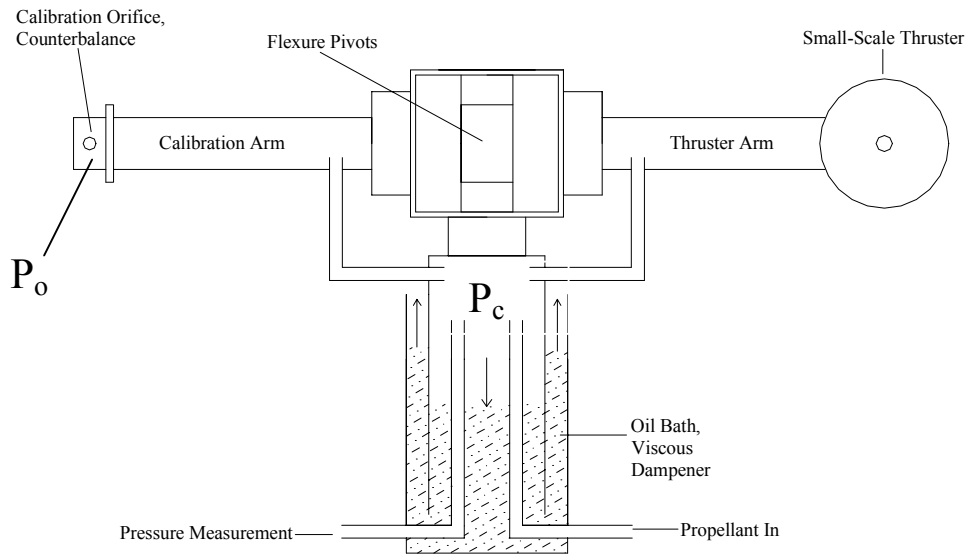


Figure 3: Schematic of thrust stand oil bath acting as propellant seal and viscous dampener.

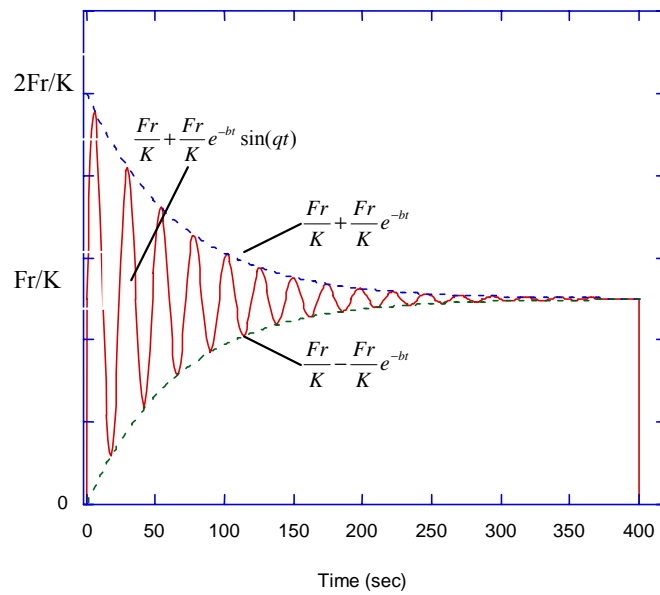


Figure 4: Deflection of a damped system with a constant thrust.

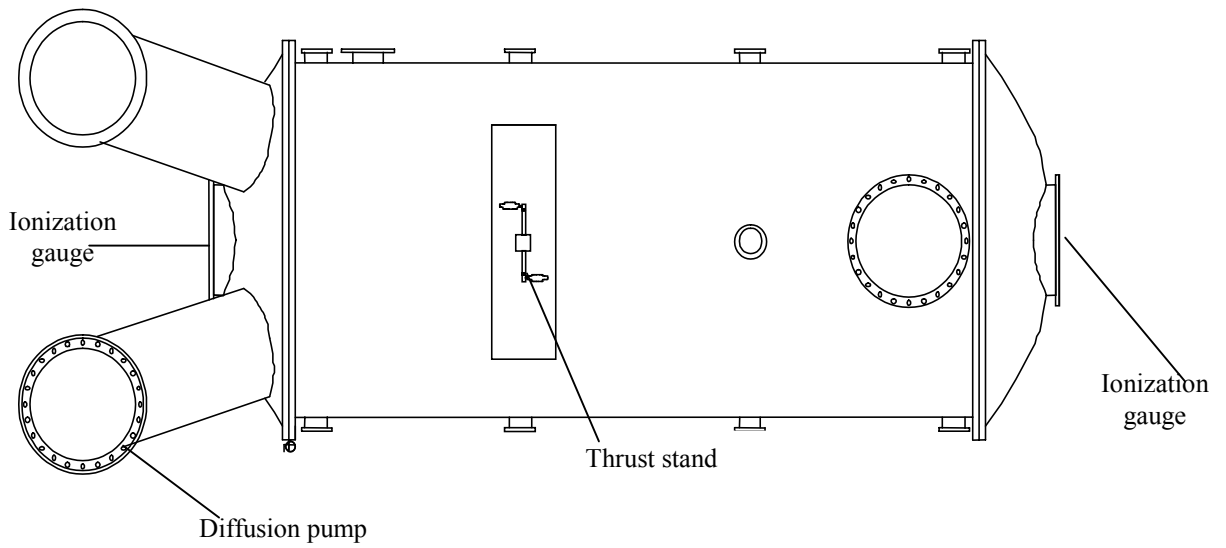


Figure 5: CHAFF-IV schematic with thrust stand location.

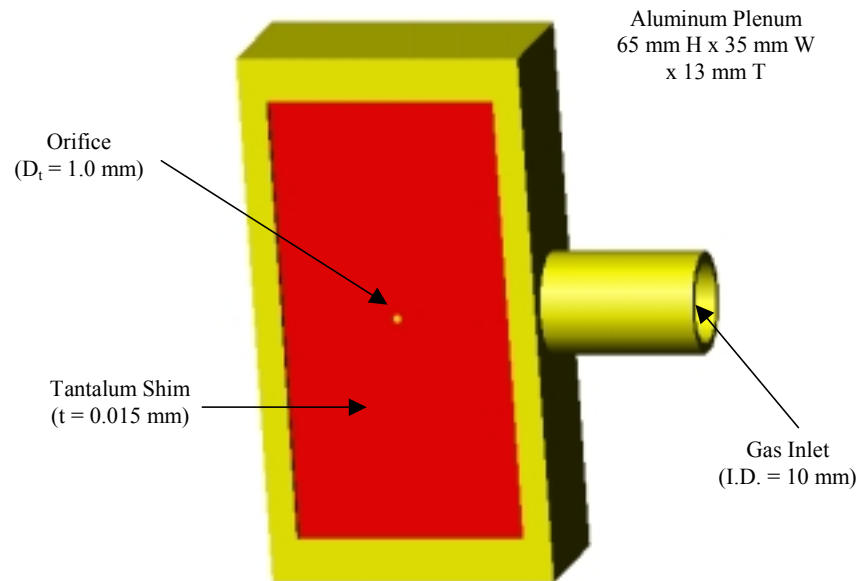


Figure 6: Orifice geometry.

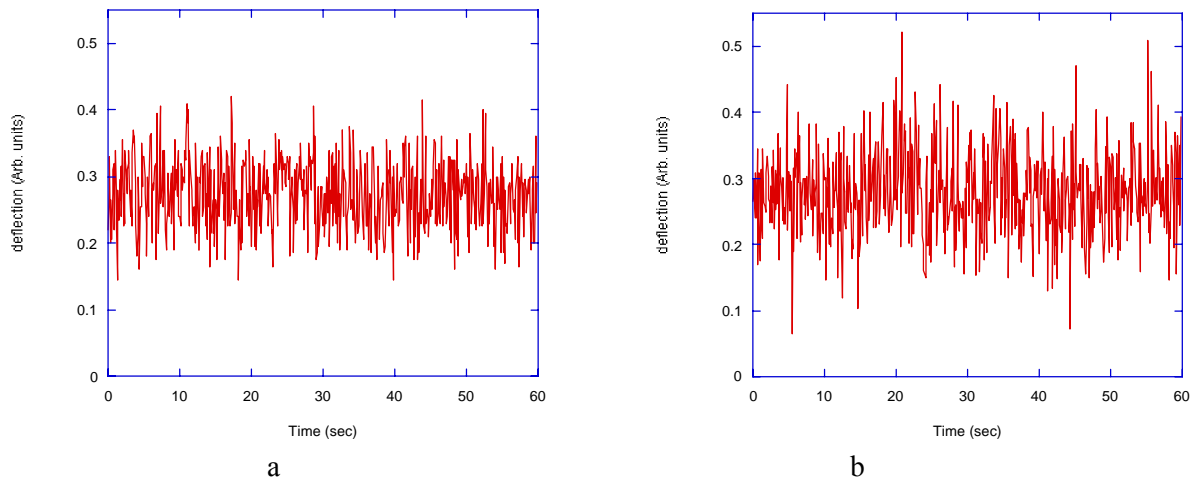


Figure 7: a) Bit noise produced by 24-bit data acquisition system. b) Bit noise from data system and environmental noise from the LVDT connected to the nNTS.

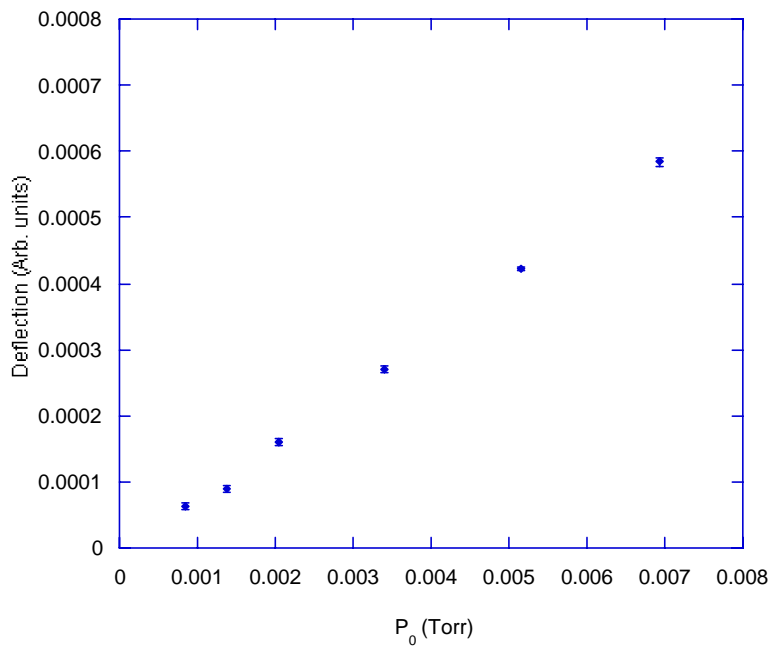


Figure 8: Deflection as a function of stagnation pressure for helium.

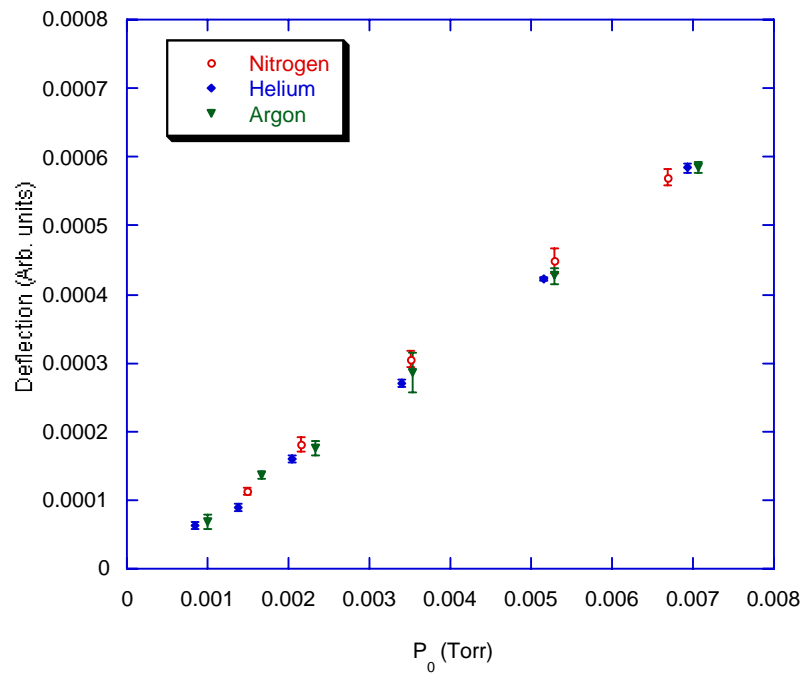


Figure 9: Deflection as a function of stagnation pressure for nitrogen, helium, and argon.

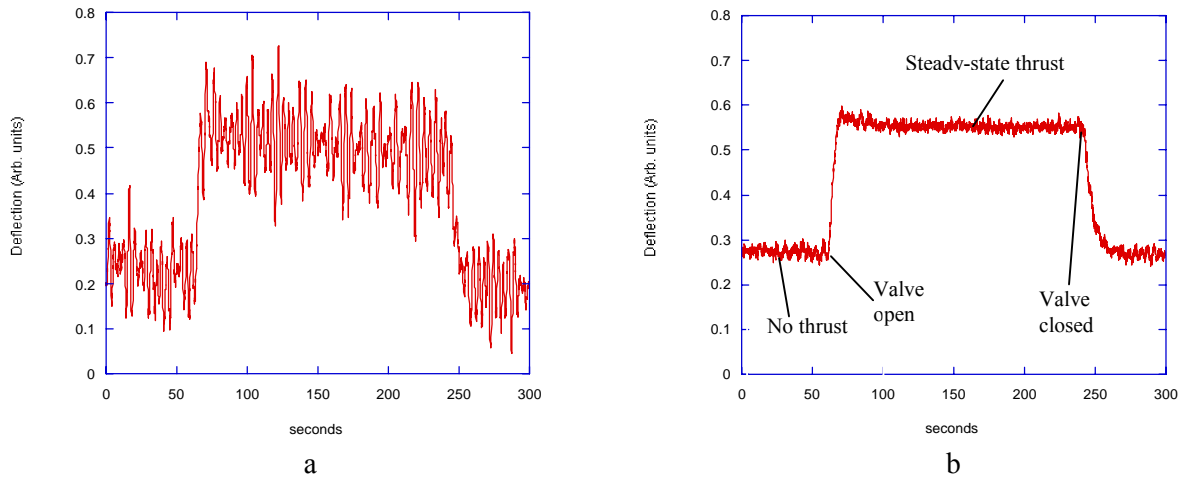


Figure 10: a) Thrust stand trace for nitrogen with $P_0 = .007$ Torr with one arm extension. b) Thrust stand trace for nitrogen with $P_0 = .007$ Torr with both arm extensions.

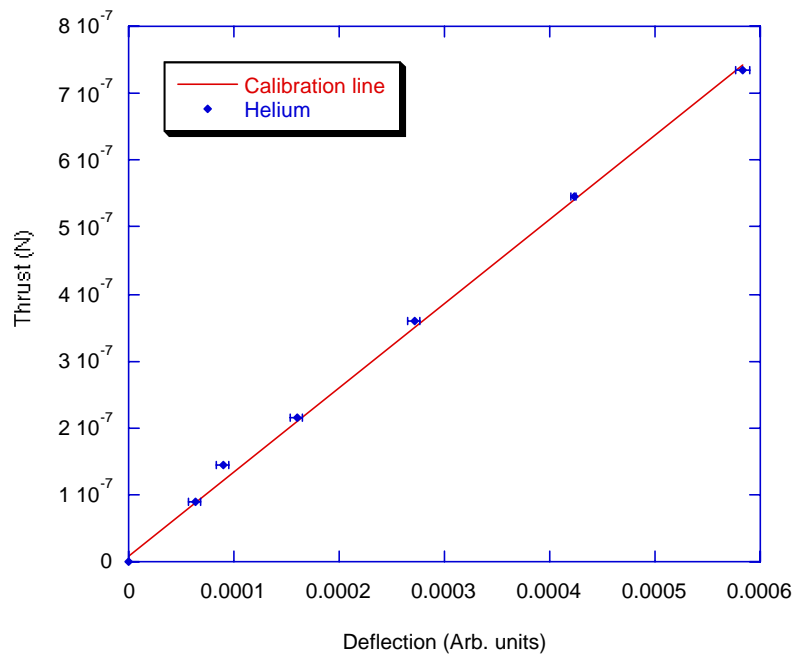


Figure 11: Calibration line derived from DSMC thrust versus experimental deflection for free molecule helium flow.

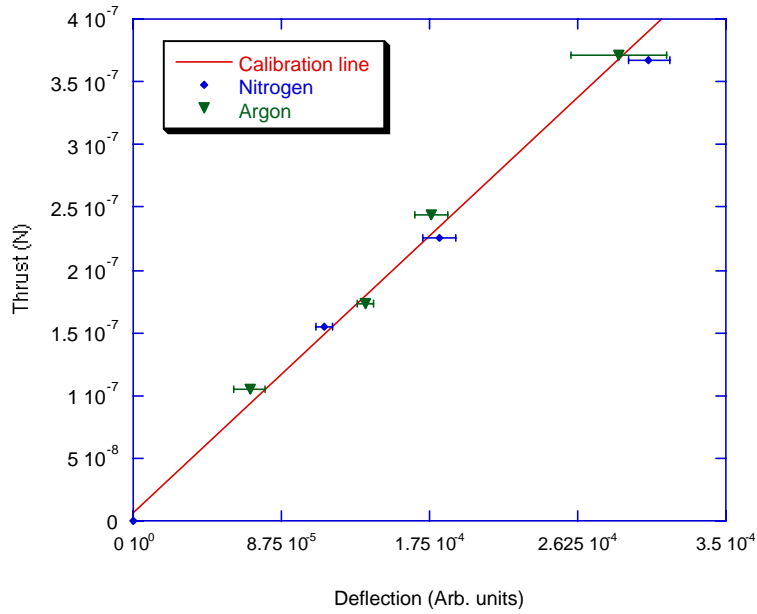


Figure 12: Calibration line with analytically derived thrust versus experimental deflection for nitrogen and argon.

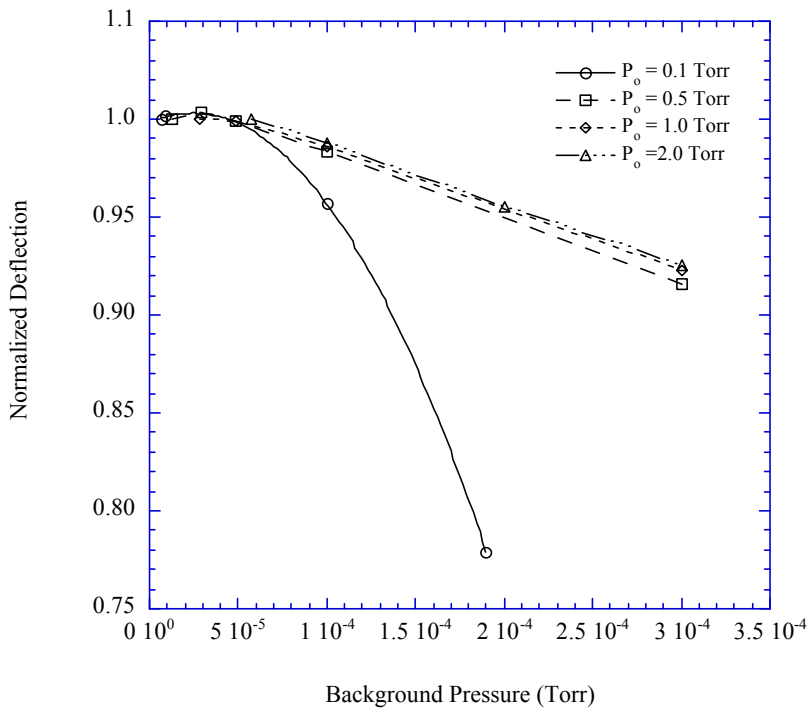


Figure 13: Normalized deflection versus CHAFF-IV background pressure for nitrogen flow at various stagnation pressures.